Thermochimica Acta, 96 (1985) 169–187
Elsevier Science Publishers B.V., Amsterdam – Printed in The Netherlands

THERMOCHEMISTRY OF COAL OXIDATION

M.S. MATYJASZCZYK *

Central Mining Institute, Plac Gwarków 1, 40–951 Katowice (Poland)

R. PRZELIORZ

Technical University of Silesia, Graniczna 16, 40-017 Katowice (Poland)

(Received 5 June 1985)

ABSTRACT

Five types of Polish bituminous coal of different grades were analysed using, simultaneously, thermogravimetric analysis (TGA), differential thermogravimetry (DTG), differential thermal analysis (DTA) and evolving gas analysis (EGA) to investigate the non-isothermal coal oxidation. The TGA, DTG and DTA curves, together with EGA, provided parameters which characterize the tendency of a given coal towards oxidation. The TGA and EGA parameters can also be used to approximate the specific active surface area of coal in reaction with oxygen. Due to the negative effects of coal oxidation, such as self-oxidation, an inhibitor was proposed and tested by analysis of the above specified thermoanalytical curves and EGA.

INTRODUCTION

Thermal analysis, using thermogravimetric analysis (TGA) and differential thermogravimetry (DTG) is an important tool for the investigation of solid state thermal decomposition [1]. Therefore, it can play an important role in the analysis of coal oxidation reactions. In addition, TGA and DTG are widely used in the proximate (content of water, volatile matter and ash), mineral content and heating value analysis of coal [2]. Nevertheless, the adaptation of TGA as a standardized method for proximate analysis must await the development of statistical data resulting from interlaboratory testing on a variety of fossil fuels [3]. Thermogravimetry, when coupled with thermomagnetometry, forms the so-called thermomagnetogravimetry (TMG) which is very helpful during investigations of content and transformations of iron compounds in thermal reactions [4]. Speed, accuracy, reproducibility and flexibility of the above-mentioned thermoanalytical methods deserve special attention.

* Correspondence address: Zamiejska 17/71, 03-580 Warszawa, Poland.

0040-6031/85/$03.30

Differential thermal analysis (DTA) of coal characterizes the heat effect of thermal decomposition, transformation and oxidation (if a thermal treatment takes place in an oxygen atmosphere). In appropriate experimental conditions (an oxidizing-mixture flow and heating rate), the DTA curve of coal resembles a "W"-shape, formed by pyrolysis and secondary carbonization bands, both exothermic and separated by the endothermic effect assigned to plastic changes in coal [5].

Coupling of a thermobalance sample-chamber with a gas chromatograph leads to the qualitative and quantitative analysis of evolving gases (EGA).

The present work shows the TGA, DTG and DTA curves, together with EGA, registered simultaneously during non-isothermal oxidation of different grades of bituminous coals, in order to find the tendency of these coals towards oxidation. The thermoanalytical curves supplied a series of parameters which characterize a given coal reactivity with oxygen. In order to lower this reactivity and decrease its exothermic heating effect, an inhibitor was used on the most active coal—the lowest grade of coal—and its efficiency was tested by the analysis of thermoanalytical curves and EGA.

Results of these investigations are of great importance for early detection of endogenic mine and pile fires, and in coal conversion processes, where the coal reactivity with oxygen is one of the criteria for its utilization in gasification processes. The Polish coal-mining industry reaches greater and greater depths [6] and looks for new methods of early mine-fire detection. Therefore, high hopes are attached to this type of investigation.

EXPERIMENTAL

Measurements were performed on the French thermoanalyser Setaram Model GDTD16, coupled with the gas chromatograph.

First, introductory measurements were performed to choose the coal powder grain size, the heating rate and the composition of the oxidation mixture.

To ensure an almost chemical control of the oxidation reaction and the possibility of comparing the different coal-grade results, a grain size of 0.06–0.075 mm was chosen.

The heating rate was 5.5°C min^{-1} in the temperature range 20–800°C.

A helium/5.5 vol.% oxygen oxidizing mixture was used to ensure the simultaneous registration of oxidation products, carbon monoxide and carbon dioxide (for the coal sample in the dry state) and methane (for moist samples as received) together with oxygen, using the same attenuation scale on the gas chromatograph. The mixtures helium/2.7 vol.% oxygen, helium/7.7 vol.% oxygen and air were also tested, initially. The flow rate of the oxidizing mixture was kept at 12 ml min^{-1}.

The sample was loaded into a crucible made of 90% platinum and 10% rhodium (v/v) and pure aluminium oxide was used as a reference.

Mass-change measurements were done with accuracy: $\pm 9.6 \times 10^{-4}$ g and 4×10^{-5} g for introductory and remaining measurements, respectively.

A catharometric detector (hot wires) and two chromatographic columns at 60°C in series, filled with Porapak Q (for carbon dioxide detection) and a molecular sieve (for oxygen, nitrogen and carbon monoxide detection), respectively, were used. Helium was used as the carrier gas at a flow rate of 55 ml min^{-1}. In each case, 2 ml of the gaseous reaction mixture were carried by the flow of oxidizing mixture to the sampling loop of the analyser and injected into the gas chromatograph every 3 min. Thus, the measurements of TGA, DTG and DTA curves were instantaneous and continuous, while EGA was discontinuous and delayed for about 6 min due to the time necessary for the emitted gases to arrive in the sampling loop of the analyser.

The activation energy of the overall reaction of pyrolysis and oxidation was calculated from the well-known equation of Freeman and Corroll [7]

$$\frac{-\frac{E}{2.203R}\Delta\frac{1}{T}}{\Delta \log W_r} = -n + \frac{\Delta \log \frac{dw}{dt}}{\Delta \log W_r} \quad (1)$$

where E is the activation energy; R is the gas constant; T is the temperature; $W_r = W_c - W$, where W_c is the mass loss at the end of the reaction and W is the mass loss at time t; dw/dt is the rate of mass loss; n is the reaction order.

RESULTS AND DISCUSSION

The results of the present work are closely related to the experimental conditions under which they were obtained. A change of grain size, composition of oxidizing mixture or heating rate leads to different results.

Table 1 presents the results of proximate and ultimate analyses.

Figure 1 shows typical TGA, DTG and DTA curves, and EGA for sample Marcel 2A. The curves in Fig. 1 are called "typical" because they present all characteristic elements visible on curves from other coals, i.e., the shape is similar but the position of bands in relation to the temperature axis or the relative band intensity may be different.

TGA and EGA

A TGA curve may be divided into three temperature regions, which are associated with different processes taking place in a given coal sample during non-isothermal heat treatment in an oxidizing atmosphere (Fig. 1). The first region, ca. 100°C, is assigned to the evaporation of water. The second

TABLE 1

Coal analysis

[D = Dymitrov, U = Unknown, M = Marcel, W = Walbrzych, W^a = water in air-dried sample, A = ash, V = Volatiles, Q_c = heat of combustion, Q_t = heating value, RI = Roga index, SI = swelling index, S_t = total sulphur, C = carbon, H = hydrogen, S_c = combustible sulphur, $(O+N)_d$ = oxygen + nitrogen, daf = dry ash free, PN = Polish Norms, Int. = International Classification]

Sample	W^a (%)	A^a (%)	V^a (%)	Q_c^a (kJ kg^{-1})	Q_t^a (kJ kg^{-1})	RI	SI	S_t^a (%)	C^a (%)	H^a (%)
D	3.18	5.65	25.81	30405	29475	14	1	0.35	78.03	3.89
U	1.35	1.93	28.17	34453	33272	67	7.5	0.53	85.26	4.50
M2A	1.45	2.51	32.41			65	7.5			
W2	0.56	3.82	18.08	34436	33507	46	8	1.49	86.99	4.18
W3	0.81	10.25	10.95	31585	30811	0	0		81.48	3.44
W1	0.77	2.69	6.76	34382	33637	0	0	0.85	89.98	3.32

Sample	S_c^a (%)	$(O+N)_d^a$ (%)	V^{daf} (%)	Q_c^{daf} (kJ kg^{-1})	S_c^{daf} (%)	C^{daf} (%)	H^{daf} (%)	$(O+N)_d^{daf}$ (%)	Type	
									PN	Int.
D	0.31	8.94	28.31	33348	0.34	85.59	4.27	9.80	32.1	711
U	0.48	6.48	29.13	35621	0.50	88.15	4.65	6.70	34.2	533
M2A			33.75						34.2	633
W2	1.42	3.03	18.91	36015	1.49	90.97	4.37	3.17	36	333
W3	0.54	3.48	12.31	35512	0.61	91.61	3.87	3.91	41	200
W1	0.83	2.41	7.00	35613	0.86	93.20	3.44	2.50	42	100

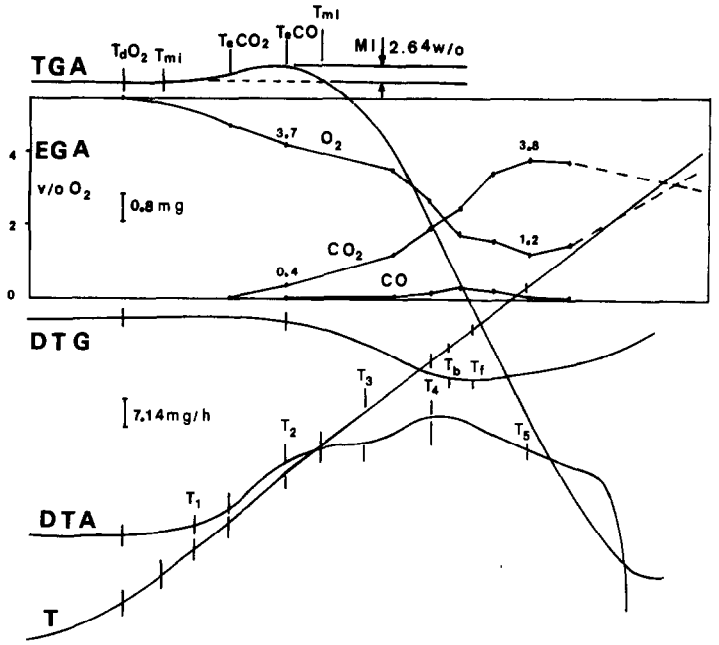

Fig. 1. Typical course of thermoanalytical curves TGA, DTG, DTA and EGA for Marcel 2A coal. Parameters: standard conditions (grain size 0.06–0.075 mm, 5.5 vol.% oxygen in helium, 5.5°C min^{-1}), DTA 100 μV, T 10 mV.

represents the mass increase and ranges from the temperature of mass increase (T_{mi}) to the temperature of mass loss (T_{ml}). The third temperature region starts at T_{ml} and represents a sudden mass loss which continues until the sample mass reaches the ash level. The values of sample mass at T_{mi} and T_{ml} are equal. The values of T_{mi}, T_{ml} and the weight percent mass increase, MI, are characteristic for a given grade of coal.

Most of the coals were investigated in the dry state, therefore, the mass loss due to moisture evaporation was small and further attention will be focused, primarily, on the region T_{mi}–T_{ml} and MI itself.

In addition, on the TGA curve, the following temperatures taken from EGA were marked: T_dO_2, temperature at which the oxygen concentration in the oxidizing mixture starts to drop; T_eCO_2, temperature at which carbon dioxide starts to evolve; T_eCO, temperature at which carbon monoxide starts to evolve; T_eCH_4, temperature at which methane starts to evolve (for moist, as received, coals) (see Figs. 4A–C).

The parameters from TGA for all the coals investigated are shown in Table 2. Comparison of these parameters indicates that the T_{mi}–T_{ml} band is located at higher temperatures and MI is higher for high grades of coal (i.e., Walbrzych 1 and 3) than for low grades (i.e., Dymitrov, "Unknown"). It is related, undoubtedly, to the lower activity of high grades of coal during oxidation, which, in turn, is related to their structure. High grades of coal are

TABLE 2

Thermoanalytical and dilatometric parameters

[U4A, 4B and 4C = "Unknown" in Figs. 4A, 4B and 4C, respectively; MeOH = methanol; b.a. = boric acid, T_{mi} = temperature of mass increase on the TGA curve; T_{ml} = temperature of mass loss; MI = mass increase; $T_b - T_f$ = temperature region of the highest mass loss rate on the DTG curve; R_{max} = maximum overall reaction rate; E = activation energy; T_1, T_2, T_3, T_4 and T_5 = approximate location of beginning and maximum of pyrolysis band, endothermal band minimum, maximum and end of the second carbonization band, respectively, on the DTA curve; a = contraction; b = dilatation; TI = softening temperature; TII = contraction temperature; TIII = dilatation temperature; T_dO_2 = temperature of oxygen drop in oxidizing mixture in EGA; T_eCO_2, T_eCO = temperature of evolution of carbon dioxide and carbon monoxide in EGA; vw = very weak peak]

Sample	Mass (mg)	Thermal analysis					
		TGA			DTG		
		T_{mi} (°C)	T_{ml} (°C)	MI (wt.%)	$T_b - T_f$ (°C)	R_{max} (mg h^{-1})	E (kcal mol^{-1})
D	20.05	178	390	1.79	537–598	14.28	21.6
D + MeOH + + 3 g/100 ml b.a.	17.00	mass loss at 73 and 166°C			540–588	10.9	20.02
D + MeOH	17.00	196	385	1.19	534–570	15.7	–
D + H_2O + + 3 g/100 ml b.a.	17.00	242	363	1.4	524–608	14.28	12.6
D + H_2O	17.12	147	385	1.8	530–578	16.4	11.62
D ox.air 24 h 155°C	17.14	–	243	0	510–564	14.28	20.42
M2A	17.00	166	385	2.64	544–585	15.5	27.10
W2	14.13	147	447	3.39	588–627	13.58	37.26
W3	17.24	270	462	2.32	588–627	14.28	34.12
W1	17.93	231	478	2.23	598–627	15.7	33.2
U	17.00	240	400	1.4	560–588	14.9	17.05
U4A	28.00	120	460	2.57	498–676	39.9	14.8
U4B	28.49	–	370	–	508	44.26	
U4C	29.25	220	426	1.1	500	35.7	

Sample	Thermal analysis								Dilatometry					S ($m^2\ g^{-1}$)
	DTA					EGA								
	T_1 (°C)	T_2 (°C)	T_3 (°C)	T_4 (°C)	T_5 (°C)	T_dO_2 (°C)	T_eCO_2 (°C)	T_eCO (°C)	a (%)	b (%)	TI (°C)	TII (°C)	$TIII$ (°C)	
D	178	374	437	520	676	230	248	–						112
D + MeOH + + 3 g/100 ml b.a.	184 isothermal effect reduced	385	447	530	–	100	271	385						
D + MeOH	196	358	457	514		128	280	400						
D + H_2O + + 3 g/100 ml b.a.	140 isothermal effect reduced			529		113	299	573 vw						
D + H_2O		353	426	520		147	265	385						
D ox.air 24 h 155°C		353	437	521		243	243	395						
M2A	220	340	437	520	650	115	260	341	26	28	360	399	426	165
W2	240	385	447	550	618	240	320	610	24	1	406	442	466	212
W3	270	350	457	563	700	293	331	529						145
W1	437	560	666	723	798	270	330	560						139
U	220	374	437	530		154	288	385	28	29	365	407	437	88
U4A	120	460/578	676	780	924		254	518						160
U4B		400				184	370	608						
U4C		457/503	666				288	457						69

more ordered and contain lower amounts of aliphatic components, which are more active in oxidation than aromatic structures. Therefore, such processes as the mass increase, related to adsorption of oxygen from the oxidizing mixture whose oxygen concentration then decreases and carbon dioxide shows up on the gas chromatograph recorder, take place at higher temperatures for high grades of coal.

Before proceeding to the explanation of why *MI* is higher for high grades of coal, one should define it more precisely to be able to appreciate its value.

In Fig. 1, *MI* is the maximum net mass increase of sample (in wt.%) as a result of two processes: adsorption of oxygen and desorption of evolving carbon dioxide (temperature of evolution of carbon monoxide is usually higher than temperature of *MI*). From T_{mi} onwards, the mass increases to its maximum value (*MI*), which suggests that sorption prevails over coal oxidation to carbon dioxide. Above the temperature at which the mass increase reaches its maximum value, the mass decreases, which indicates that oxidation to carbon dioxide and carbon monoxide starts to dominate in the overall reaction. The oxygen stored so far in the coal mass becomes active and forms carbon dioxide and carbon monoxide at higher temperatures, with the support of oxygen from the oxidizing mixture. Thus, the sum of a surface area taken by the adsorbing oxygen and a surface area left by desorbing carbon dioxide at the temperature of *MI* gives the maximum active surface area of a given coal for the adsorption of oxygen. For example, for Marcel 2A (Fig. 1), from *MI* 2.64 wt.%, initial sample mass 0.017 g (without a temperature correction) and assuming 0.166 nm^2 to be the area of an oxygen molecule in a monolayer [8], the active surface area becomes 165 $m^2\ g^{-1}$ (Table 2). From the evolution of carbon dioxide, assuming that each carbon dioxide molecule has consumed one molecule of oxygen, one can obtain 3.5 $m^2\ g^{-1}$ which, combined with the surface area from *MI*, gives 168.5 $m^2\ g^{-1}$. This is a large surface area and there is a high content of volatile matter in this sample (Table 1), so pyrolysis which starts at 150°C for some coals [2a] could have an influence on it. According to Schlyer and Wolf [9], at low temperatures such as 21°C, a coal particle of the order used in the present work oxidizes in the outer layer. At 150°C, there is no gradient of oxygen/carbon ratio throughout the particle. Hence, we can assume that at the beginning of non-isothermal oxidation, a particle is oxidized in the outer layer to the order of a few microns and at the *MI* temperature it is fully saturated with oxygen. There is no gradient of oxygen concentration throughout the particle. This would confirm that the *MI* represents the maximum saturation of coal mass (surface and bulk) with oxygen. A small percentage of sorption sites are strong adsorption sites, amounting to 10^{14}–$10^{19}\ g^{-1}$ coal [9].

The above surface area estimated from *MI*, is of the same order as the specific surface areas obtained by other methods [10,11], e.g., carbon dioxide adsorption at different temperatures or X-ray small angle diffraction, for a

similar grade of coal. Before performing our calculations, the oxygen balance between loss and increase of carbon dioxide in the oxidizing gas mixture, and the mass increase on the TGA curve at a given time interval (corresponding to the time of EGA measurement) were checked and good agreement was obtained.

Consequently, one may say that *MI* provides information on the total maximum surface and bulk saturation with oxygen, taking place from the beginning of non-isothermal oxidation up to the *MI* temperature, while the surface estimated from the oxygen loss in the oxidizing mixture at a given reaction time (shown by EGA, Fig. 1) about the surface taking part directly in the reaction at a given temperature (oxygen loss is monitored discontinuously, see Experimental section). For example, for Marcel 2A at ca. *MI* temperature, oxygen losses amounted to 1.76 vol.%, which corresponds to 5.6×10^{19} active sites/g coal. 0.36 vol.% of carbon dioxide was formed, which corresponds to 1.2×10^{19} active sites/g coal which are directly involved in the oxidation process. It agrees very well with Schlyer's number of strong active sites in coal oxidation of young coals, cited above.

In general, the problem of coal surface area measurements using thermogravimetry requires further analysis and simultaneous comparison with specific surface areas estimated by other adsorption methods. It would be useful, also, to perform isothermal thermogravimetric analysis at given temperatures for better evaluation of coal reactivity with oxygen. The above discussion merely draws one's attention to the possibility of thermogravimetric surface area measurements on coals. This possibility seems specially attractive in a light of the fact that adsorption of carbon dioxide at 298 K, for example, was found not to be a relevant reactivity normalization parameter in the gasification of coal chars [12]. Oxygen chemisorption capacity at 375 K from the air (0.1 MPa) was found to be a valid index of char reactivity and, therefore, gives an indication, at least from a relative viewpoint, of the concentration of active sites of carbon in a char.

The maximum mass increase (*MI*) introduced in the present work, is a type of oxygen sorption capacity, without substantial oxidation to carbon dioxide and carbon monoxide, at temperatures from room temperature to the temperature corresponding to *MI*. It shows that a large role can be played by thermogravimetry when trying to measure the active surface area of coal during reactions with gaseous reactants.

The *MI* comparison of different coals in Table 2 shows that *MI* is higher for high grades of coal. It takes values of 1.4 and 1.79 wt.% for low grades of coal ("Unknown" and Dymitrov, respectively) and up to 3.39 wt.% for high grades of coal (e.g., Walbrzych 2). In addition, the *MI* phenomenon takes place at higher temperature for high grades of coal. The higher temperature at which *MI* occurs, combined with its higher value, suggests once more, that the high grades of coal are less active in the oxidation reaction and, therefore, require a higher degree of surface saturation with oxygen and a

higher temperature to produce carbon dioxide and carbon monoxide. Similar results concerning *MI* were obtained by Mitra and Raja [13], who used thermogravimetry to find the so-called ignition temperature of coal. It seems that the ignition temperature corresponds to the temperature of *MI* (Fig. 1) in the present work. Mitra and Raja do not present their curves, nor do they show how to read the exact position of *MI* on the temperature scale. In this paper, the T_{mi}–T_{ml} band, including *MI*, is very diffuse, therefore, the authors have chosen to report the values of T_{mi} and T_{ml}, rather than *MI*.

In addition, Mitra and Raja [13] use a powder of the grains which is passed through a 0.212-mm sieve. The present work reports results on 0.06–0.075-mm powders which should keep the oxygen transport effect to a minimum and ensure an almost chemical control of reaction at least for the higher temperatures at which coal particles are saturated with oxygen [9]. The narrow range of grain size should help to eliminate the differences in grain size distribution in different coal samples and, in this way, enable a meaningful comparison to be made of results from different coal samples. Both problems, the overall grain size and its range, were discussed by Karsner and Perlmutter [8] and, according to their analysis, a grain size of 0.06–0.075 mm should satisfy both conditions.

The EGA curve, presented in Fig. 1, shows changes in the oxygen, carbon dioxide and carbon monoxide concentrations in the oxidizing mixture as the temperature of non-isothermal heat treatment increases. The decreasing concentration of oxygen is always associated with the increasing concentration of carbon dioxide and then carbon monoxide, and vice versa. The carbon monoxide concentration is much lower than that of carbon dioxide and starts to increase at higher temperatures. The characteristic temperatures of oxygen drop (T_dO_2) and evolution of carbon dioxide and carbon monoxide (T_eCO_2, T_eCO) are marked on the TGA curves and specified in Table 2. The evolution of carbon dioxide and carbon monoxide starts at lower temperatures for low-grade coals than for high-grade coals, which is related directly to the change in position of the T_{mi}–T_{ml} range, discussed earlier.

DTG

DTG curves generally exhibit a broad band corresponding to the maximum mass loss on TGA curves above the T_{ml} temperature. The DTG band represents the resultant reaction rate of mass loss, which consists of all possible reactions occurring in a given sample, including oxidation and pyrolysis. From TGA and DTG curves, one may calculate the maximum resultant reaction rate and activation energy from Eqn. 1 (see Experimental section). The values of these reaction rates and activation energies are given in Table 2, together with temperatures at the beginning and end of band minimum on the DTG curve (T_b and T_f, respectively). The values for the activation energies of the overall reaction agree well with those of Karsner

and Perlmutter [8] (25, 10, 18 and 33 kcal mol^{-1} for activation energy for carbonic gas formation, physical adsorption, physical desorption and chemical adsorption of oxygen, respectively). It appears that the overall reaction has a higher activation energy for high-grade coals, which confirms their lower reactivity with oxygen. The location of the T_b–T_f band on the DTG curve shifts toward higher temperatures with an increase of coal grade, which is connected directly with the course of the TGA curves, on which T_{m_1} and T_{m_2} also take higher values for higher-grade coals.

Before a broad negative band of mass loss on the DTG curve, a small and very diffuse band of mass gain can be seen. It corresponds to *MI* on the TGA curve with the maximum reaction rate from 1.8 to 3.5 mg h^{-1}.

DTA

A DTA curve represents the thermal effect associated with non-isothermal oxidation and thermal decomposition of the coal structure. It consists of two diffuse exothermic bands separated by an endothermic band. Table 2 presents temperatures T_1, T_2, T_3, T_4 and T_5, which are approximate positions of the beginning and maximum of the first exothermic band, endothermic minimum, and maximum and end of the second exothermic band, respectively, on the temperature scale (see also DTA curves in Figs. 1–4). An assignment of the exact location of the DTA bands is difficult due to their diffuse character.

According to the previous interpretation of DTA curves, taken during pyrolysis of gas-coals [5], the band at T_2 corresponds to the beginning of intensive thermal decomposition of organic substances. Surface oxidation and dehydrogenation contribute to the exothermic character of this band. The endothermic band which follows, with a minimum at about T_3, is a result of decomposition, polycondensation of pyrolysis products and phase transformation. It is located in the region of coal plasticity in which molecules agglomerate and, in this way, increase the thermal conductivity of a sample. At T_4, the exothermal effect becomes dominant once more, and is usually described as coming from a secondary carbonization, assisted by separation of hydrogen still remaining in peripheral aromatic rings. Above T_4, the DTA curve declines due to the endothermal character of further ordering of the hexagonal coal structure as well as a decrease of coal mass resulting from intensive oxidation. Comparing the mass loss at T_4 on the TGA curve with the volatile matter content from proximate analysis (Table 1), a good agreement can be seen which further supports the interpretation of the T_4 band as belonging to the secondary carbonization taking place after the volatile matter has disappeared.

However, measurements in helium show, for Dymitrov coal, one very diffuse band in place of two previous bands for pyrolysis and secondary carbonization, with the secondary carbonization band being dominant (Fig.

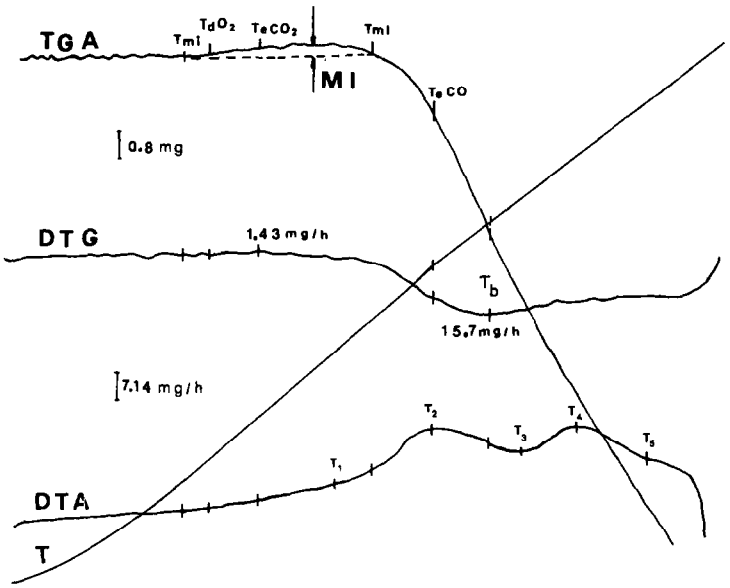

Fig. 2. Thermoanalytical curves for Walbrzych 1. Parameters as in Fig. 1.

3A). The maximum reaction rate negative peak on the DTG curve is sharper and located in the same region as in the oxidation experiment with the maximum reaction rate reduced to 2.7 mg h^{-1}. The location of this band corresponds to the maximum mass drop on the TGA curve, which does not have the *MI* effect but only a gradual mass loss with a sudden drop in the

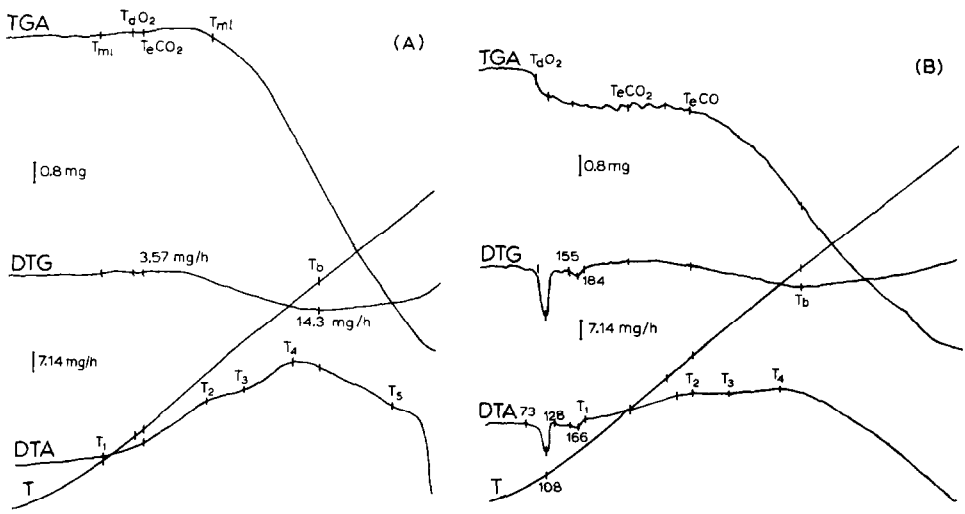

Fig. 3. (A) Thermoanalytical curves for Dymitrov coal. Parameters as in Fig. 1. (B) Thermoanalytical curves for Dymitrov coal, saturated for 24 h with 3 g/100 ml boric acid in methanol, air dried and run under standard conditions. Parameters as in Fig. 1.

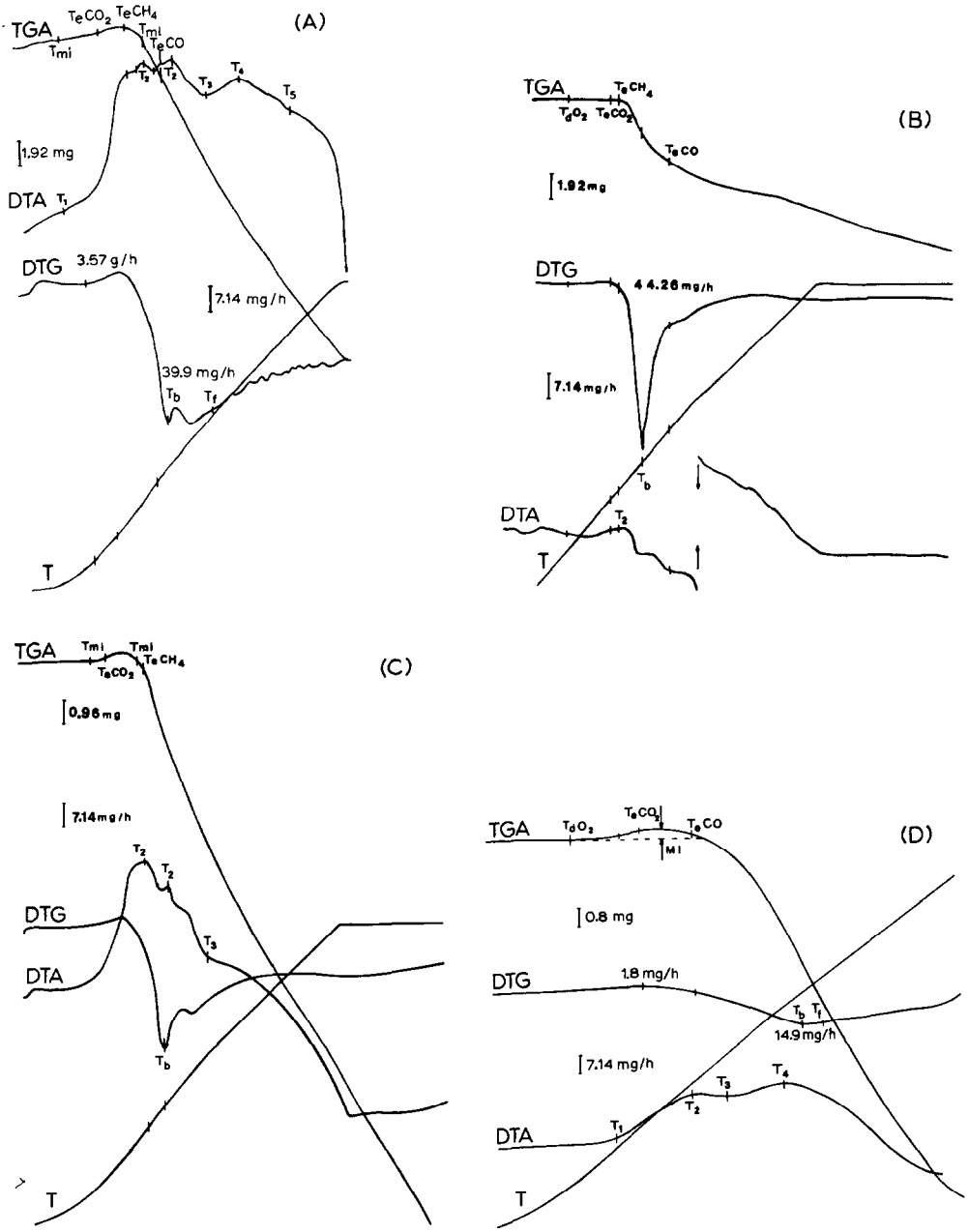

Fig. 4. (A) Thermoanalytical curves for "Unknown" (ground in mortar) run in air. Parameters: DTA 250 μV, T 20 mV, heating rate 13.5°C min^{-1}. (B) Thermoanalytical curves for "Unknown" coal of random grain distribution of the order of mm in 2.7 vol.% oxygen in helium. Parameters: DTA 100 μV, T 20 mV, heating rate 13.5°C min^{-1}. (C) Thermoanalytical curves for "Unknown" coal in 7.7 vol.% oxygen in helium, grain size as in Figs. 4A and 4B. Parameters: DTA 250 μV, T 20 mV, heating rate 13.5°C min^{-1}. (D) Thermoanalytical curves for oxidation of "Unknown" coal run under standard conditions. Parameters as in Fig. 1.

vicinity of the DTG band due to the separation of volatiles. It confirms the pyrolysis interpretation of the first band on the DTA curve and suggests that oxidation also has a lot to do with the second band—the secondary carbonization band. In the case of high-grade coal (Walbrzych 1) we see no band separation on the DTA curve, which shows a continuous drop, lack of bands on the DTG curve and a continuous gradual drop of mass on the TGA curve. In the case of non-isothermal oxidation (Fig. 2) we have two bands on the DTA curve of almost the same intensity with a deep endothermal inflection between them, a negative peak on the DTG curve and a characteristic drop after *MI* on the TGA curve. It supports, also, the above statement that oxidation plays a major role in shaping the "secondary carbonization" and "pyrolysis" bands on the DTA curve.

The endothermal inflection on the DTA curve at T_3, interpreted as the plastic region of coal, is supported by dilatometric data in Table 2 for plastic coals. *T*I, *T*II and *T*III, being the softening, maximum contraction and dilation temperature, respectively, lie near T_2, T_3 and T_4 on the DTA curve for plastic coals.

In general, one may say that the DTA curve represents the thermal effect of coal decomposition, with the oxidation effect superimposed on it. Differences are clearly visible in the behaviour of different grades of coal. The above-mentioned pyrolysis and secondary carbonization bands with superimposed oxidation, shift towards higher temperatures for higher-grade coals; differences reach 200°C in some cases (Table 2). The differences in band intensity are visible for different coals; for higher-grade coals, e.g. Walbrzych 1 (Fig. 2), the pyrolysis band at T_2 increases in intensity to equal the intensity of the secondary carbonization band, which dominates for low-grade coals. It is probably connected with the structure of the high-grade coals, in which the role of the aliphatic portion in the turbostatic structure is smaller. The higher degree of ordering in the planar aromatic structure of the high-grade coals is characterized by the stronger binding energies, hence, the higher heat effect of the pyrolysis band. These same factors (structure, degree of ordering and coal composition) cause the DTA, DTG and TGA bands to shift towards higher temperatures for high-grade coals. Additionally, the maximum reaction rate on the DTG curve for high-grade coals shifts to lower temperatures, closer to the location of the location of the pyrolysis band on the DTA curve (see Figs. 1 and 2), which points to an increased pyrolysis role in the overall reaction. On the DTA curve, the intensity of the exothermal bands is smaller for the high-grade coals (Figs. 1 and 2), i.e., Marcel 2A and Walbrzych 1, respectively, which suggests a lower self-ignition tendency with the high-grade coals.

Degree of coal oxidation

After running the non-isothermal oxidation experiment on the Dymitrov coal, previously oxidized in air for 24 h at 155°C, a lack of *MI* was observed

which suggests that the critical amount of oxygen needed for the saturation of active centres was supplied to the sample during initial oxidation. Non-isothermal oxidation provided the activation energy to form carbon dioxide and carbon monoxide, their desorption from the coal surface and further oxygen to fill newly available active centres in order to make the oxidation continuous. The temperature of oxygen loss from the oxidizing mixture equals, in this case, T_{ml} and T_eCO_2, and the mass loss takes place here at lower temperatures. Apart from these differences, the shapes of the DTG and DTA curves for oxidized and non-oxidized coal from the Dymitrov mine are similar.

Inhibitors

Coal powders were saturated for 24 h and then dried to the air-dry state with solutions of boric acid in water and methanol. Boric acid was chosen as an inhibitor due to its mild interaction when in contact with living organisms. It was tested as an inhibitor of coal auto-oxidation by Kaiser and Ghosh [14], who noticed an increase in the coal ignition point as a result of its application. Boric acid is also used to combat fires.

In the present work, the inhibitor was applied to the lowest-grade coal—Dymitrov. The non-isothermal oxidation measurements were also performed on the coal saturated with water and methanol, and air-dried in both cases, to test the solvent influence on the inhibiting process.

In the case of coal saturated with boric acid in methanol (Fig. 3B), a mass drop was observed on the TGA curve which was assigned to the evaporation of methanol at 73°C. At about 166°C, H_3BO_3 transforms into HBO_2, which is reflected on the DTG curve by a mass loss peak, and on the DTA curve by an endothermal peak. The peak assigned to methanol evaporation has its equivalent on the DTG and DTA curves. It is interesting to note that both endothermal peaks (at 73 and 166°C) on the DTA curve appear in the region where, previously, in the uninhibited sample undergoing non-isothermal oxidation, the exothermal increase at the start of the pyrolysis band was taking place. Additionally, both exothermal bands, which nevertheless appear in the inhibited coal sample, are substantially reduced. It was this exothermal character of the oxidation reaction which led, usually, to self-ignition of coal. As we can see, the saturating inhibitor and solvent go through endothermal transformations which consume an excess of heat from the oxidation and, by doing so, inhibit further oxidation.

The boric acid in water did not cause such visible mass losses on the TGA curve and peaks on the DTG and DTA curves. However, the DTA exothermal peaks were considerably reduced. This could be related to a higher degree of penetration into the coal by the methanolic solution, due to its higher dissolving ability of the coal structure than for the water solution.

The above effects of endothermal peaks and the reduced character of the exothermal effect in non-isothermal oxidation did not take place on samples saturated with water or methanol.

Further, oxidation runs with pure solid powder of boric acid and with a mixture of 50 wt.% Dymitrov coal and 50 wt.% boric acid were done to check if peaks which appeared on DTA and DTG curves, taken from Dymitrov coal saturated with a 3 g/100 ml solution of boric acid in methanol or water, came from the solute. The 166°C peak for boric acid was confirmed and two new endothermal peaks showed up for boric acid curves, as well as for the boric acid–Dymitrov mixture. Those new peaks represent a large endothermal effect at 140 and 196°C on the DTA and DTG curves, and mass losses on the TGA curves. On Dymitrov–boric acid thermographs, the three peaks appeared at 134, 172 and 196°C, respectively. They all contributed, probably, to the reduction of exothermal bands on the DTA curve taken from Dymitrov coal saturated with a 3 g/100 ml solution of boric acid in methanol and water, and were not visible due to the small concentration in solution.

In the case of EGA, a substantial reduction of T_dO_2 takes place, as well as an increase of T_eCO_2 for inhibited samples (Table 2 and Fig. 3). The reasons for an earlier consumption of oxygen are not known. The increased temperature of evolution of carbon dioxide may be connected with the inhibiting effect.

Results versus experimental conditions

At the beginning of this section (Results and Discussion), it was emphasized that the results of this work should be treated as being closely related to the experimental conditions under which they were obtained. To support this statement, Figs. 4A, B and C were presented, where non-isothermal oxidation was performed under different conditions. Samples were not air-dried here, hence, water reacting with carbon forms small amounts of methane.

Figure 4A presents non-isothermal oxidation of "unknown" sample with air, heating rate 13.5°C min^{-1} and grain size of the order of mm (few irregular grains taken from a sample ground in mortar). For comparison, the curves for the above standard conditions (0.06–0.075 mm grain size, 5.5 vol.% oxygen in helium as oxidizing mixture and 5.5°C min^{-1} heating rate) are presented in Fig. 4D.

The TGA curve in Fig. 4A looks similar to that with a heating rate of 5.5°C min^{-1} and 5.5 vol.% oxygen in helium (Fig. 4D), however, *MI* is rather big (2.57 wt.%), suggesting a surface area of ca. 160 $m^2\ g^{-1}$, close to that of Marcel 2A under standard conditions. Undoubtedly, a major role was played here by pyrolysis and increased oxygen concentration. Under the same conditions of grain size and heating rate, but with a reduced oxygen

concentration to 2.7 vol.% in helium (Fig. 4B), there is a shortage of oxygen which is used entirely in reaction and no *MI* shows up.

The DTA curve in Fig. 4A presents two bands, with the major role played by the pyrolysis band. The course of this curve is similar to the DTA curves of Wang and Shou [5] despite the fact that the heating rate is almost three times higher. The pyrolysis band splits into two, which, supposedly, represent two phases of pyrolysis. After the first phase, ordering takes place together with an additional adsorption of oxygen (see the small band in the "minimum valley" on the DTG curve) and is followed by the second phase of pyrolysis and oxidation. The DTA curve is shifted to higher temperatures, which could be explained by an increased heating rate and slower oxygen sorption. Nevertheless, intensive oxidation and decomposition determines the domination of the first two bands over the second carbonization band. Under standard conditions of grain size (Fig. 4D), grains are smaller and such intensive decomposition does not take place, hence, the intensity of the second carbonization band is higher than that of pyrolysis.

The DTG curve shows a maximum positive increase of the order of 3.57 mg h^{-1}, corresponding to the maximum oxygen adsorption on the TGA curve. Later, one sees a deep minimum described above. Maximum reaction rate equals 39.9 mg h^{-1}. EGA shows additional evolution of methane at $T_eCH_4 = 374°C$.

Figure 4B presents the oxidation results of the same sample with 2.7 vol.% oxygen in helium and a 13.5°C min^{-1} heating rate. There is no *MI* on the TGA curve. DTG takes the form of one well-defined peak at 508°C, corresponding to a rapid mass loss on the TGA curve. The high value of the maximum reaction rate (44.26 mg h^{-1}) compared with previous reactions, suggests that active sites are blocked when there is an excess of oxygen. EGA points to the complete oxygen consumption during oxidation, which gives 8 m^2 g^{-1} for the active surface area. This value is, of course, too low due to a lack of oxygen which, in larger amounts, would also chemisorb on the surface and react. The DTA curve has a very diffuse character with a falling tendency above 508°C, which corresponds to the minimum on the DTG curve and a large mass loss on the TGA curve. The pyrolysis peak dominates and the second carbonization peak is not visible, which suggests that most of its intensity comes from oxidation taking place earlier in this experiment. EGA shows the evolution of methane at $T_eCH_4 = 400°C$.

Figure 4C, for the same sample as in Figs. 4A and B, shows oxidation in 7.7 vol.% oxygen in helium with a 13.5°C min^{-1} heating rate. Again, *MI* is observed (ca. 1.1 wt.%) giving 69 m^2 g^{-1} for the surface area, which is smaller than in Fig. 4A due to the smaller oxygen concentration. We see similarities with Fig. 4A in the case of the pyrolysis band split and its intensity being higher than for the second carbonization band. EGA shows the evolution of methane at $T_eCH_4 = 457°C$.

The surface area of "Unknown" after oxidation under standard condi-

tions, with $MI = 1.4$ wt.% (Table 2, Fig. 4D), amounted to 88 $m^2\ g^{-1}$. The sample in Fig. 4C consisted of coal pieces, hence, its surface area is smaller. In addition, on the DTA curve, the pyrolysis band is reduced in comparison with Figs. 4A, B and C to a lower intensity than that of the second carbonization band. (This was discussed above, in the analysis of Fig. 4A.) On the DTG curve, the peak of maximum reaction rate is preceded by a small band of mass gain with reaction rate 1.8 mg h^{-1} corresponding to *MI*.

Sample "Unknown" was taken as unknown, and after proximate and ultimate analyses the thermoanalytical parameters were measured. The coal type according to Polish classification, found on the basis of volatile content, Roga index, dilatometry and heat of combustion (Table 1), was that of Marcel 2A. The parameters of thermal reactions have a lot of similar features (see Table 2 and Figs. 1 and 4D).

CONCLUSIONS

Summing up the above results and discussion, one may definitely state that thermogravimetry, derivatography and differential thermal analysis in connection with evolving gas analysis provide parameters characterizing the tendency towards oxidation for coals of different degrees of metamorphism. The set of such parameters includes: T_{mi}, T_{ml}, *MI*, T_dO_2, T_eCO_2 and T_eCO on the TGA curve and EGA; T_b and T_f on the DTG curve; T_1–T_5 on the DTA curve.

Furthermore, from the *MI* and by EGA, one may estimate the maximum active surface area for a given coal in the adsorption reaction of oxygen, as well as the maximum active surface area (or the number of strong active sites) in the oxidation reaction at a given temperature.

From the *MI*, conclusions concerning the degree of coal oxidation can also be drawn.

The course of TGA, DTG and DTA curves, along with EGA, is an important indicator of the efficiency of oxidation inhibitors.

All these findings point to further possibilities of thermoanalysis applications in coal reactivity research, apart from the proximate and mineral content analyses.

ACKNOWLEDGEMENTS

The research described in the present work was fully financed by the Central Mining Institute, which supported measurements performed in the Institute of Material Engineering, Technical University of Silesia by R.P.

We thank all those authors who sent us copies of their papers, from which we have cited several references here (refs. 1, 2, 4, 5, 9).

REFERENCES

1 L. Reich and S.S. Stivala, Thermochim. Acta, 62 (1983) 129; 61 (1983) 361 and references therein.
2 a R.J. Rosenvold, J.B. Dubow and K. Rajeshwar, Thermochim. Acta, 53 (1982) 321. b C.M. Earnest and R.L. Fyans, Perkin-Elmer Thermal Analysis Application Study, Vol. 32, 1981. c C.M. Earnest, W.P. Brennan and R.L. Fyans, 2nd Proc. Eur. Symp. Thermal Analysis, 1981, p. 517. d J.W. Cumming and J. McLaughlin, Thermochim. Acta, 57 (1982) 253. e P. Baur, Power, 127 (3) (1983) 91.
3 J.P. Elder, Fuel, 62 (1983) 580.
4 M. Hyman and M.W. Rowe, New Approaches in Coal Chemistry, ACS Symp. Ser., No. 169, American Chemical Society, Washington, DC, 1982, p. 389.
5 Z. Wang and J.K. Shou, Prep. Pap. Am. Chem. Soc. Div. Fuel Chem., Symp., 25 (4) (1980) 171.
6 M. Swiss, World Coal, 8 (6) (1982) 118.
7 E.S. Freeman and B. Corroll, J. Phys. Chem., 62 (1958) 394.
8 G.G Karsner and D.D. Perlmutter, Fuel, 61 (1982) 29 and references therein.
9 D.J. Schlyer and A.P. Wolf, New Approaches in Coal Chemistry, ACS Symp. Ser., No. 169, American Chemical Society, Washington DC, 1981, p. 87; Proc. 4th Int. Conf. on Nuclear Methods in Environmental and Energy Research, Columbia, MO, April 14–17, 1980.
10 Z. Spitzer and L. Ulicky, Fuel, 55 (1) (1976) 21.
11 P.L. Walker and K.A. Kini, Fuel, 44 (6) (1965) 453.
12 L.R. Radovic, P.L. Walker, Jr. and R.G. Jenkins, Fuel, 62 (7) (1983) 849.
13 P.K. Mitra and K. Raja, J. Mines, Met. Fuels, 30 (8) (1982) 416.
14 F.M. Kaiser and C. Ghosh, J. Mines, Met. Fuels, 31 (1983) 283.